Bioorganic Chemistry 87 (2019) 638–646

Contents lists available at ScienceDirect

Bioorganic Chemistry

journal homepage: www.elsevier.com/locate/bioorg

Discovery of new inhibitors against both NF-κB and osteoclastogenesis from in-house library with α, β-unsaturated-enone fragment

Chao Zhao[a], Dane Huang[a,b], Ruyue Li[b,d], Jiake Xu[e], Qiong Gu[a,*], Jun Xu[a,c,*]

[a] Research Center for Drug Discovery, School of Pharmaceutical Sciences, Sun Yat-sen University, Guangzhou 510006, People's Republic of China
[b] Guangdong Province Engineering Technology Research Institute of T. C. M., Guangdong Provincial Key Laboratory of Research and Development in Traditional Chinese Medicine, Guangzhou 510095, People's Republic of China
[c] School of Biotechnology and Health Sciences, Wuyi University, 99 Yingbin Road, Jiangmen 529020, People's Republic of China
[d] Guangzhou University of Chinese Medicine, Guangdong Second Traditional Chinese Medicine Hospital, Guangzhou 510095, People's Republic of China
[e] Molecular Laboratory, School of Biomedical Science, University of Western Australia, Perth, Western Australia, Australia

ARTICLE INFO

Keywords:
NF-κB inhibitors
α,β–unsaturated enone
Osteoclastogenesis
RANKL

ABSTRACT

The α,β-unsaturated-enone contained natural products have been reported showing NF-κB inhibition effect. It is well known that NF-κB inhibitors can also be used to inhibit osteoclastogenesis. In a continual discovery new agents for anti-osteoclastogenesis, 8 different type compounds with α,β-unsaturated-enone fragments from our in-house library were evaluated for NF-κB inhibition and anti-osteoclastogenesis. Experimental results indicated five compounds exhibited inhibition of NF-κB signal pathway. Among them, one compound ((*E*)-2-(4-fluorobenzylidene)-3,4-dihydronaphthalen-1(2*H*)-one, **6a**) simultaneously inhibits both osteoclastogenesis and NF-κB signal pathway. Furthermore, 12 compounds with similar scaffold with **6a** were tested for anti-osteoclastogenesis. As a result, 9 compounds inhibited both NF-κB and osteoclastogenesis. Among them, compound **6b** is the most potent inhibitor against NF-κB (IC_{50} = 2.09 μM) and osteoclast differentiation (IC_{50} = 0.86 μM). Further studies show that compound **6b** blocks the phosphorylation of both p65 and IκBα, and suppresses NF-κB targeted gene expression without interfering MAPKs and PI3K/Akt signal transduction pathways. This study demonstrates that we can identify promising synthesized compounds with new scaffolds as therapeutic solutions against osteoclastogenesis inspired by the privileged fragment derived from natural leads.

1. Introduction

Bone remodeling is regulated by both osteoblasts and osteoclasts [1]. When bone resorption exceeds bone formation, it results in osteoporosis. Osteoclasts are generated from receptor activator of nuclear factor-κB ligand (RANKL) induced bone-marrow-derived macrophages (BMMs). RANKL is a member of tumor necrosis factor (TNF) family, and expressed by bone stromal cells, osteoblasts and T lymphocytes [2,3]. When RANKL binds to its receptor RANK, nuclear factor-κB (NF-κB) signal transduction pathways will be activated to regulate the osteoclast-associated genes expression, including cathepsin K, matrix metal loprotease-9 (MMP-9) [4], nuclear factor of activated T cells c1 (NFATc1) [5], and tartrate-resistant acid phosphatase (TRAP) [6]. These proteins play important roles in regulating osteoclast survival, differentiation, and function [7]. Therefore, blocking the activity of NF-κB signal transduction pathway can stop osteoclastogenesis.

NF-κB is the protein complex of RelA (also known as p65), p50, p52, RelB, and c-Rel. In osteoclast, NF-κB is usually formed by IκBα, p65, and p50 [8]. When RANKL binds to RANK, TNF receptor (TNFR)-associated factor 6 (TRAF6) is recruited and induces a trimeric IκB kinase (IKK) complex phosphorylated by ATP binding. This in turn leads to the phosphorylation of IκBα and its degradation by 26S proteasome. The degradation of IκBα allows p65 and p50 heterodimer to be phosphorylated and translocated into nucleus [9]. This results in transcription of targeted genes, hence increasing cellular differentiation, function and resistance to apoptosis [10].

Known NF-κB osteoclastogenesis inhibitors, such as parthenolide [11], AKBA [12], curcumin [13], and andrographolide [14], have been discovered from nature (Fig. 1). α, β–Unsaturated enone (Fig. 1) is the privileged fragment for these compounds, which are usually inhibitors for both NF-κB and osteoclastogenesis. The privileged fragment is reported that can form covalent bond with the Cys46 of IKKβ [15], the Cys38 of p65 [16] or the Cys62 of p50 [17,18].

In order to discover new scaffold osteoclastogenesis inhibitors, the

* Corresponding authors at: Research Center for Drug Discovery, School of Pharmaceutical Sciences, Sun Yat-sen University, Guangzhou 510006, People's Republic of China.
E-mail addresses: guqiong@mail.sysu.edu.cn (Q. Gu), junxu@biochemomes.com (J. Xu).

https://doi.org/10.1016/j.bioorg.2019.03.066
Received 8 January 2019; Received in revised form 16 February 2019; Accepted 24 March 2019
Available online 28 March 2019

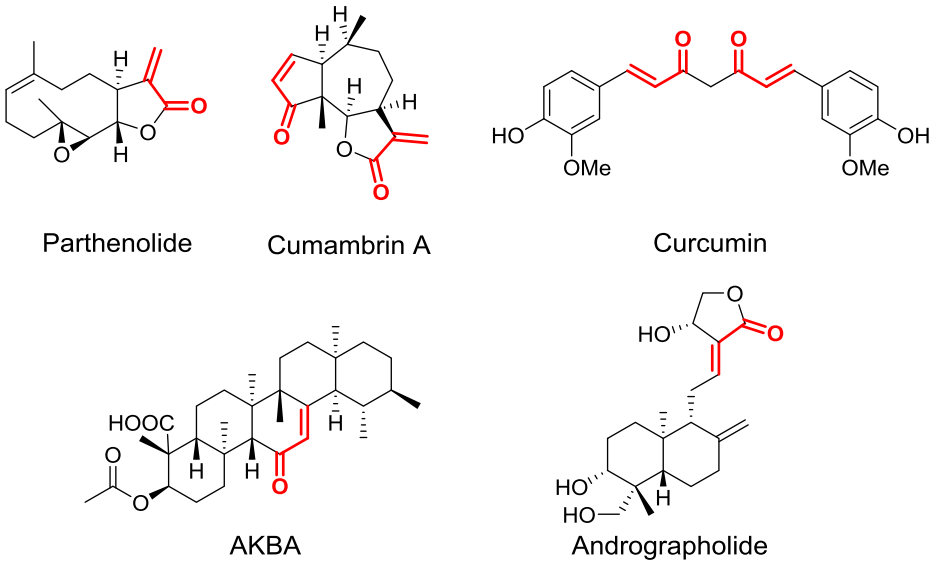

Fig. 1. The known osteoclastogenesis inhibitors discovered from natural products.

privileged fragment α, β–unsaturated enone contained compounds were screened from our in-house library for lead identification. Then, cell-based biological assays were performed to validate the screening results to identify new inhibitors against both NF-κB and osteoclastogenesis.

2. Results and discussion

2.1. Screening anti-osteoporosis compounds from in-house library

Using α, β–unsaturated enone as a query, we retrieved our in-house compound library, and resulted in 81 compounds which were classified into 8 scaffold groups. Based on scaffold diversity, we selected 8 compounds (one compound per scaffold group) for NF-κB inhibition validation (Table 1). Experimental results indicated that 5 compounds (**1**, **2**, **4**, **5**, **6a**, and **8**) inhibited NF-κB. Compound **6a** is the most potent NF-κB inhibitor (IC_{50} = 1.65 μM) in RANKL treated RAW264.7 cells. Osteoclast differentiation inhibitory assays revealed that only compound **6a** significantly reduced RANKL-induced osteoclast differentiation in a dose-dependent manner (Fig. 2). These results suggested that **6a** simultaneously inhibited NF-kB and osteoclastogenesis.

2.2. Identifying anti-osteoclastogenesis compounds with new scaffold

To identify more active compounds with the scaffold of compound 6**a**, we selected 12 additional **6a** derivatives from the in-house library to validate their NF-κB inhibitory activity (Table 2). Experimental results showed 9 of them are NF-κB inhibitors, and compound **6b** is 4-times more active than compound **6a**. As shown in Table 2, when hydrophobic groups were replaced at R_3, such as, SMe (**6c**), OBn (**6d**) and, NEt_2 (**6e**), the compound would lose NF-κB inhibitory activity. Bulky group at R_2 can significantly reduce the activity, however, a hydrophobic group at R_2 can reduce the activity more than a hydrophilic group (**6f**, **6g**, and **6h**). Enlarging A-ring can also reduce NF-κB inhibition (**6l** and **6m**).

The compounds in Table 2 inhibit both NF-κB and osteoclastogenesis without cytotoxicity, although the activities of NF-κB and osteoclast differentiation inhibition are not always consistent (**6f**, **6h–6k**, **6m**). A possible explanation is that they might interact with different targets, such as PI3K [20] and MAPK [21]. Compound **6b** is the most potent inhibitor against NF-κB (IC_{50} = 2.09 μM) and osteoclast differentiation (IC_{50} = 0.86 μM). We will further study its function and mechanism for the treatment of osteoporosis.

Table 1
Eight compounds containing α, β–unsaturated enone and their bioactivity.

Cmpd. NO.	Structures	NF-κB IC_{50} (μM)[a]	Osteoclast inhibition IC_{50} (μM)[b]
1	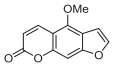	25.92 ± 4.23	> 30
2	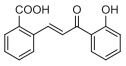	6.67 ± 0.54	> 30
3	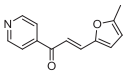	Inactive[c]	> 30
4	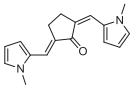	5.41 ± 1.22	> 30
5	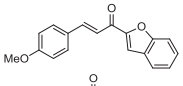	6.35 ± 1.03	> 30
6a	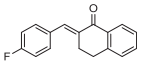	1.65 ± 2.50	8.66 ± 3.84
7	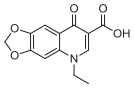	Inactive[c]	> 30
8	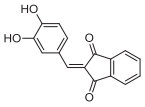	Inactive[c]	> 30
JSH23[d]	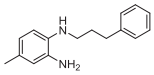	8.10 ± 0.58	7.64 ± 1.21

[a] Concentration (μM) for 50% inhibition of NF-κB activation in RANKL-induced RAW264.7 cells. The IC_{50} values are the mean ± SEM for at least three experimental determinations NF-κB.

[b] Concentration (μM) for 50% inhibition of osteoclast differentiation in RANKL-induced RAW264.7 cells. The IC_{50} values are the mean ± SEM for at least three experimental.

[c] Compounds exhibit no effect at 30 μM.

[d] JSH23 is a commonly used NF-κB inhibitor [19].

2.3. Compound 6b suppresses osteoclastogenesis and bone resorption in vitro

For further confirming the activity of compound **6b**, freshly isolated bone marrow macrophage cells (BMMs) were treated with various

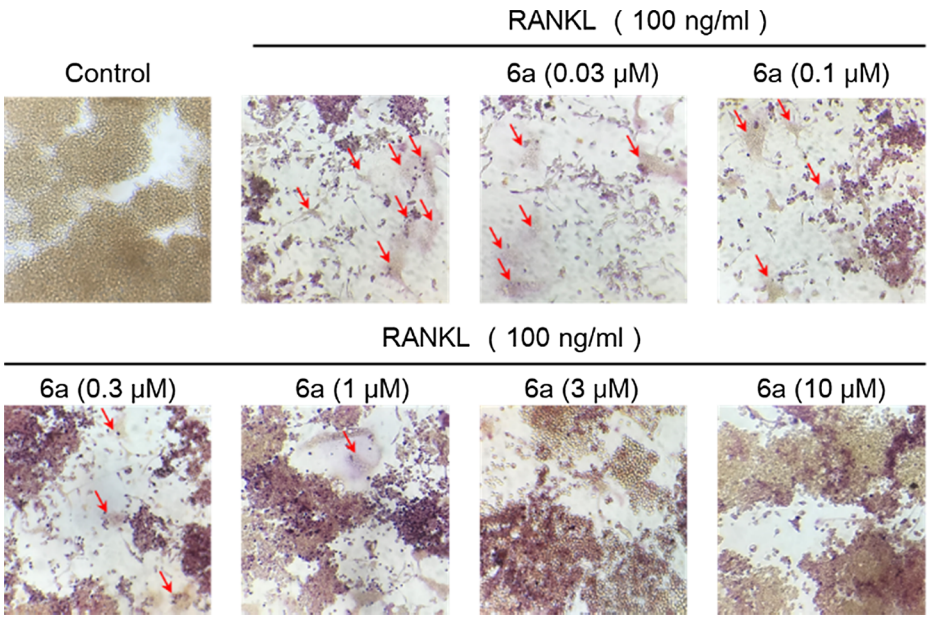

Fig. 2. Compound **6a** attenuates RANKL-induced osteoclastogensis in a dose-dependent manner. RAW264.7 cells were cultured in a 96-well plate in the presence of RANKL (100 ng/mL) and compound **6a** (0–10 μM) for 7 days and then fixed with 4% paraformaldehyde and stained for TRAP activity. Representative light microscope images showing the effect of compound **6a** on RANKL-induced osteoclast formation with morphological changes in comparison with RAW264.7 cells cultured in the absence and presence of RANKL. The TRAP-positive multinucleated cells that contain more than 3 nuclei were counted (red arrow). (For interpretation of the references to color in this figure legend, the reader is referred to the web version of this article.)

Table 2
SAR for compounds with the scaffold of compound **6a**.

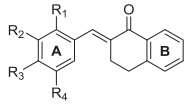

No.	R1	R2	R3	R4	NF-κB IC_{50} (μM)[a]	Osteoclast inhibition IC_{50} (μM)[b]	CC_{50} (μM)[c]
6a	−H	−H	−F	−H	8.66 ± 3.84	1.65 ± 2.50	> 50
6b	−H	−H	−OH	−H	2.09 ± 0.45	0.86 ± 1.27	> 50
6c	−H	−H	−SMe	−H	Inactive[d]	Inactive	> 50
6d	−H	−H	−OBn	−H	Inactive	Inactive	> 50
6e	−H	−H	$-NEt_2$	−H	Inactive	Inactive	> 50
6f	−H	−F	−H	−H	20.56 ± 0.79%[e]	1.89 ± 0.32	> 50
6g	−H	−Cl	−H	−H	37.79 ± 9.06%	15.99 ± 4.73	> 50
6h	−H	$-NO_2$	−H	−H	7.86 ± 1.44	1.42 ± 0.19	> 50
6i	−Cl	−H	−H	−H	18.63 ± 5.98	1.24 ± 0.79	> 50
6j	$-NO_2$	−H	−H	−H	12.23 ± 4.11	1.81 ± 0.29	> 50
6k	−H	−OH	−OH	−H	13.18 ± 4.73	1.02 ± 0.18	> 50
6l	$-NO_2$	−H	−OMe	−OMe	45.23 ± 4.32%	9.00 ± 0.94	> 50
6m	−H	$-NO_2$	−OH	−OMe	36.69 ± 4.23%	1.56 ± 0.40	> 50

[a] Concentration (μM) for 50% inhibition of NF-κB activation in RANKL-induced RAW264.7 cells. The IC_{50} values are the mean ± SEM for at least three experimental determinations NF-κB.

[b] Concentration (μM) for 50% inhibition of osteoclast differentiation in RANKL-induced RAW264.7 cells. The IC_{50} values are the mean ± SEM for at least three experimental.

[c] Concentration for 50% death of RAW 264.7 cells. The CC_{50} values are the mean ± SEM for at least three experimental.

[d] Compounds exhibited no effect at 30 μM.

[e] Percentage activity of test compounds at 30 μM in RANKL-induced NF-κB.

concentrations of **6b**. As shown in Fig. 3, compound **6b** can completely stop the osteoclast formation at 10 μM, and reduced half number of osteoclasts at 1 μM (IC_{50} = 0.91 μM). CCK8 assay analysis indicated that compound **6b** is non-cytotoxicity at the tested concentration (Fig. 3B).

Next, the effect of compound **6b** on osteoclast function was examined by using hydroxyapatite-coated plates (Fig. 3C). Compare to RANKL treated group, compound **6b** can reduced the area of hydroxyapatite resorption in dose-dependent manner (Fig. 3C and D).

2.4. Compound 6b selectively inhibits NF-κB signal transduction pathway

Both p65 and IκBα plays important roles in NF-κB signal transduction pathway. Phosphorylating p65 and IκBα can activate DNA transcription. Compound **6b** significantly reduced phosphorylated p65 (p-p65) in about 5–60 min (Fig. 4A), p65 expression level change was not observed, indicating that compound **6b** inhibited p65 activity. Similarly, the phosphorylation of IκBα (p-IκBα) was also suppressed by compound **6b** in about 5–60 min (Fig. 4B).

Besides the NF-κB signal transduction pathway, RANKL also interacts with MAPKs (ERK, JNK, and p38) and PI3K/Akt signal transduction pathway. The inhibitory effects of compound **6b** on two signal transduction pathways were evaluated by western blot experiments. As shown in Fig. 5, phosphorylation of ERK, JNK, p38, PI3K, and Akt were not changed when treated with compound **6b**. These findings demonstrated that compound **6b** inhibited osteoclast differentiation through RANKL-induced NF-κB signal transduction pathway without interfering MAPKs and PI3K/Akt signal transduction pathway.

2.5. Compound 6b inhibits osteoclastogenesis-related gene expression

The expression of TRAP, c-Fos, MMP-9, and NFATc1 is regulated by NF-κB signal transduction pathway. Therefore, their mRNA levels in RANKL-induced BMMs were examined (Fig. 6). Increased levels of TRAP, c-Fos, MMP-9, and NFATc1 were observed after RANKL treated, but these expression levels were significantly suppressed in presence of compound **6b**. These results further confirmed that compound **6b** inhibits NF-κB signal transduction pathway and reduces osteoclastogenic marker gene expression.

2.6. Compound 6b has no effect on osteoblast differentiation

Furthermore, bone morphogenetic proteins 2 (BMP-2) induced C2C12 cells were used for testing effect of **6b** on osteoblast function. As shown in Fig. 7A, **6b** did not affect the osteoblast marker alkaline phosphatase (ALP) expression when examined by ALP staining. CCK8 assay indicated **6b** is no cytotoxicity at the tested concentration (Fig. 7B).

2.7. Docking study indicates compound 6b may covalent bind with IKKβ

Since compound **6b** only affects NF-κB signal transduction pathway

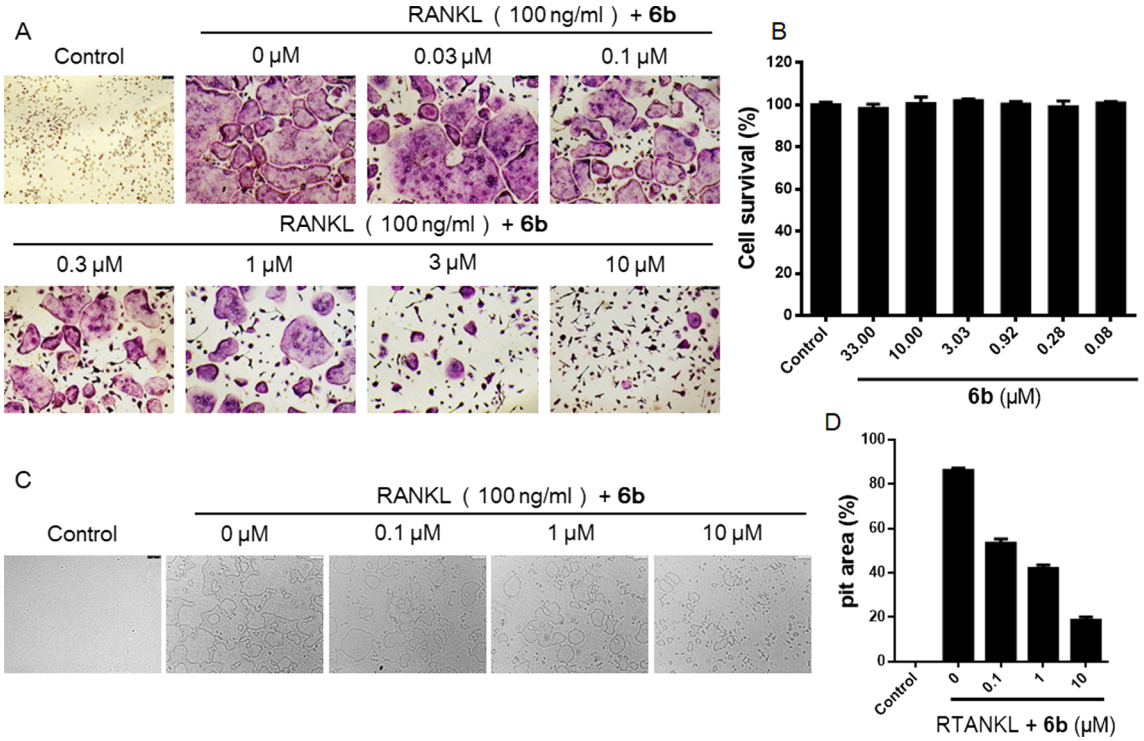

Fig. 3. (A) Compound **6b** attenuates RANKL-induced osteoclastogenesis in a dose-dependent manner. BMMs cultured in a 96-well plate in the presence of RANKL (100 ng/mL), M-CSF (30 ng/mL) and compound **6b** (0–10 μM) for 5 days were fixed with 4% paraformaldehyde and stained for TRAP activity. Representative light microscope images showing the effect of compound **6b** on RANKL-induced osteoclast formation compared with BMMs cultured in the absence and presence of RANKL and M-CSF. The TRAP-positive multinucleated cells that contain more than 3 nuclei were counted as osteoclast. (B) Compound **6b** did not affect viability of BMMs as measured by CCK8 assay. (C) Representative image of bone resorption on hydroxyapatite-coated plates. (D) Quantification of the percentage area of hydroxyapatite surface with or without **6b**.

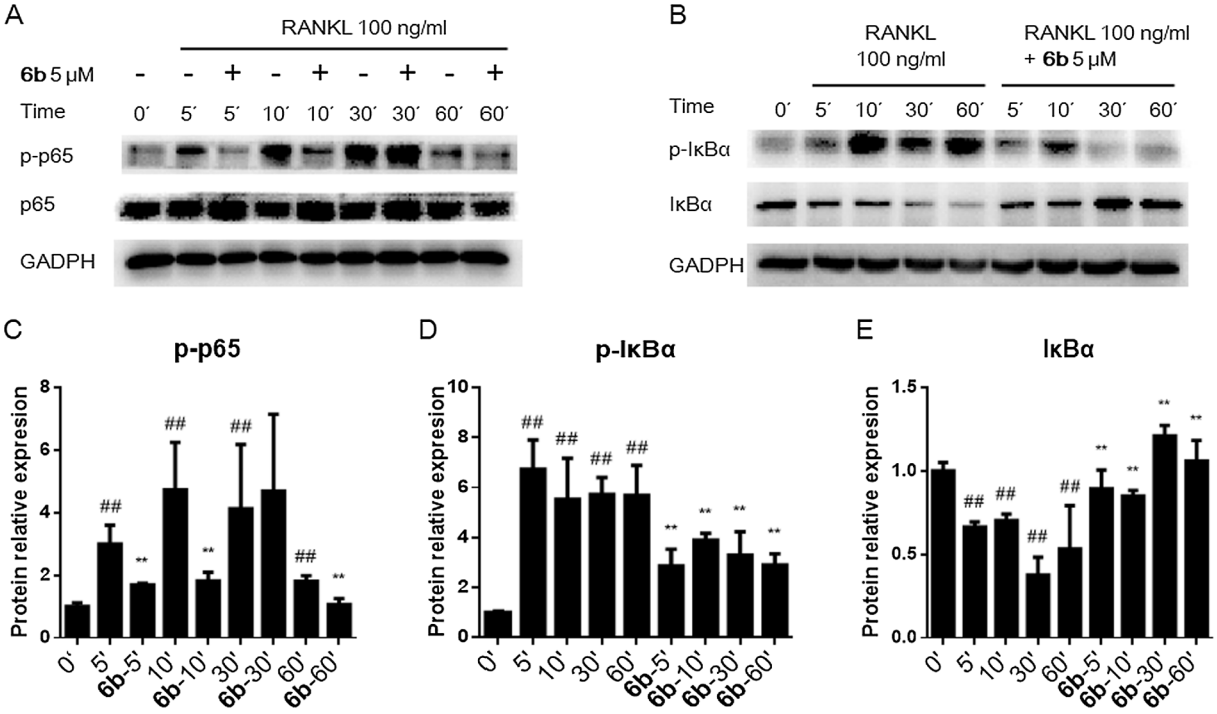

Fig. 4. Compound **6b** inhibited RANKL-induced activation of NF-κB signal transduction pathway. Compound **6b** (5 μM) was added to RAW 264.7 cell incubated in 4 h before RANKL (100 ng/mL) treated and further incubated for 5, 10, 30, and 60 min. Then the protein samples were prepared for total and phosphorylated p65 and IκBα analysis. (A, C) Western blots analysis of the effect of **6b** on p-p65, the data in blots were quantified by densitometry. (B, D and E) Western blots analysis of the effects of **6b** on p-IκBα and IκBα, the data in blots were quantified by densitometry. Results are expressed as mean ± SD of three independent experiments. $^{\#\#}$, $p < 0.01$ compared with control (0′). **, $p < 0.01$ compared with the RANKL-treated group.

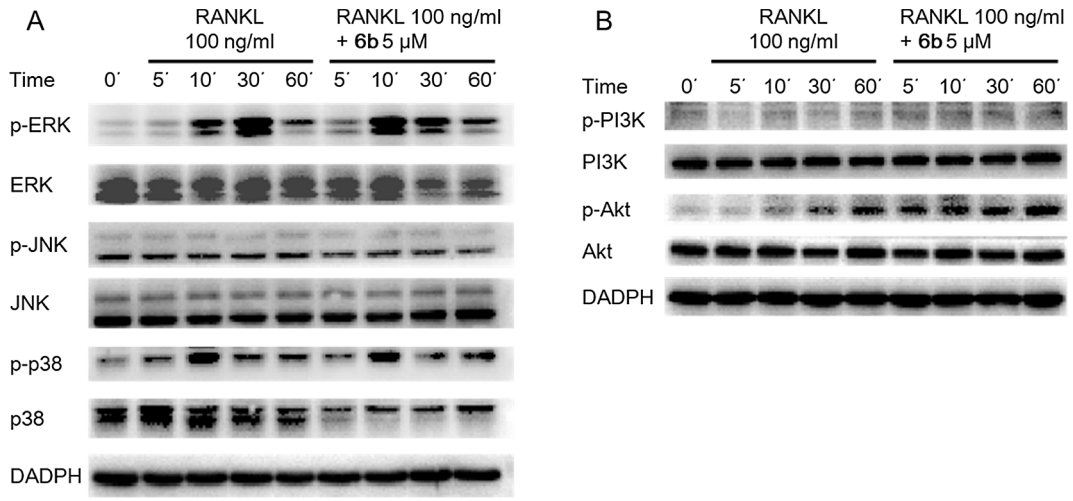

Fig. 5. Effects of compound **6b** on RANKL-induced activation of MAPK and PI3K/Akt signal transduction pathway. Compound **6b** (5 μM) was added to RAW 264.7 cell incubated in 4 h before RANKL (100 ng/mL) treated and further incubated for 5, 10, 30 and 60 min. Then the protein samples were prepared for total and phosphorylated ERK, JNK, p38, PI3K and Akt (p-ERK, p-JNK, p-p38, p-PI3K, p-Akt) analysis. (A) Effect of **6b** on p-ERK, p-JNK and p-p38. (B) Effect of **6b** on p-PI3K and p-Akt.

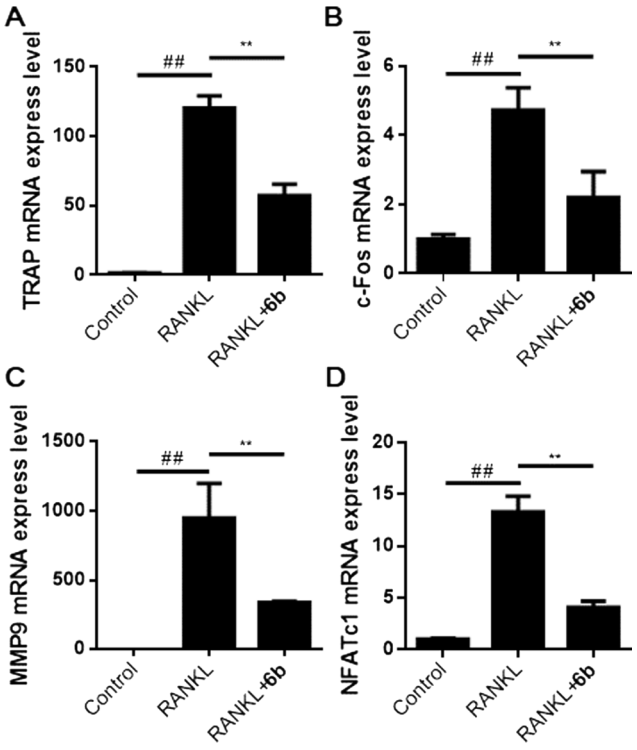

Fig. 6. Effect of compounds **6b** (5 μM) on osteoclastogenic mRNA expression. BMMs were pretreated with or without the compound **6b** for 1 h and then supplemented with RANKL (100 ng/mL) for the indicated time points. Total RNA was isolated with TRIzol, and each total RNA was used to transcribe the cDNA. The cDNA was amplified by PCR from mouse-specific primers. Results are expressed as mean ± SD of three independent experiments. $^{\#\#}$, $p < 0.01$ compared with control. **, $p < 0.01$ compared with the RANKL-treated group.

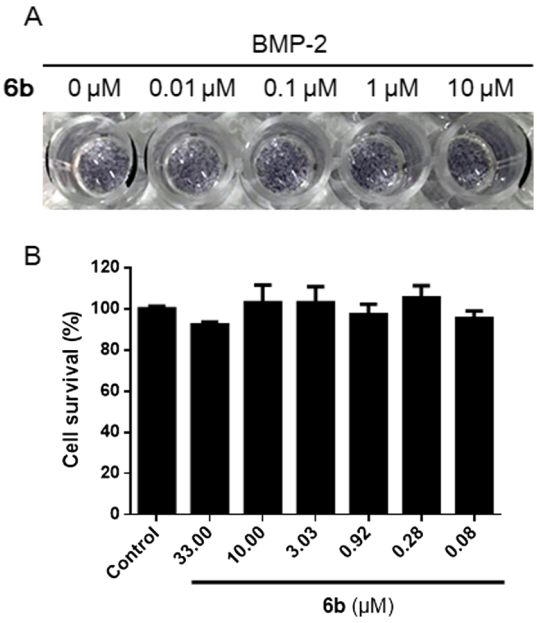

Fig. 7. (A) Effects of **6b** on BMP-2 induced C2C12 cells myoblast differentiation examined by ALP staining. C2C12 cells cells were treated with BMP-2 (10 ng/mL) for 3 days, fixed in 4% paraformaldehyde and stained for ALP activity. (B) Compound **6b** did not affect viability of C2C12 cells as measured by CCK8 assay.

and prevents the phosphorylation of p65 and IκBα at the same time, it may work on upstream protein such as IKKβ and TRAF6. α,β–Unsaturated enone may form covalent bond with Cys46 of IKKβ to inhibit NF-κB signal transduction pathway. Therefore, we propose that compound **6b** may blocks NF-κB activity through regulating IKKβ (PDB code: 3QA8). As it has been reported that Cys46, Glu49, Arg55, Trp58, Ile62, Val79, and Leu91 can form an allosteric binding pocket in IKKβ (Fig. 8A). Occupying the pocket reduces NF-κB activity [15]. Compound **6b** was docked into this binding pocket (Fig. 8B) using MOE software [22]. The dihydronaphthalenone of **6b** establishes hydrophobic interactions with Trp58, Leu91, Pro92, and Ile62. The hydroxy group at the phenol ring of compound **6b** interacts with Arg47, Glu49, and Arg55 (Fig. 8C). Compound **6b** also interacts with IKKβ via two hydrogen bindings. One is formed between carbonyl group of dihydronaphthalenone and the NH in indole ring of Trp58; another is formed between the phenol ring and Glu49 (Fig. 8C). This binding model makes the α-C of α,β–unsaturated enone in **6b** close to thiolate Cys46 (3.58 Å) and induces Michael addition reaction (Fig. 8C).

Compound **6b** was covalently docked into the binding pocket of IKKβ at Cys46 (PDB code: 3QA8) and minimized the complex energy with Amber99 force field (Fig. 9A and B). The result indicates that this ATP binding pocket is significantly altered after **6b** is covalently

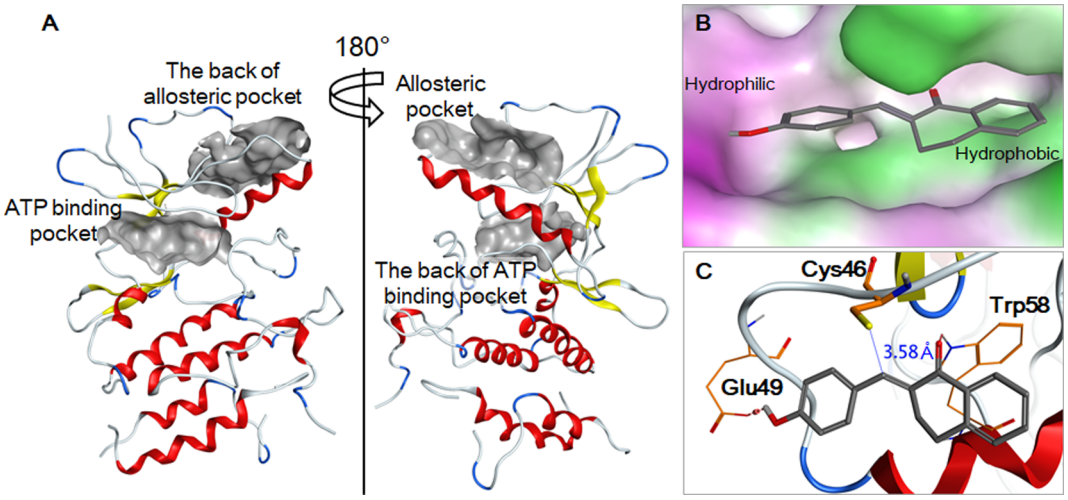

Fig. 8. (A) Allosteric pocket and ATP binding pocket of IKKβ. (B, C) The binding mode of **6b** with IKKβ. H-bonds are represented as orange dashed lines. Hydrophobicity (lipophilicity) is represented as textured colors where green is more hydrophobic, while pink is less hydrophobic. Distance are represented as blue line. (For interpretation of the references to color in this figure legend, the reader is referred to the web version of this article.)

docked: (1) Gly25 is repositioned from the original pose to the ATP chamber; (2) Asp166 is folded and caused a clash interaction with ATP; (3) the backbone carbonyl of Glu97 is rotated and the hydrogen binding with ATP is lost. Thus, the binding of ATP and IKKβ is weaken, consequently, NF-κB signal transduction pathway is interfered. This mechanism is important because IKKβ is more important to osteoclast differentiation than other homologs such as IKKα and IKKγ [23–25].

2.8. Discussion

In this study, a new scaffold of compounds was discovered to inhibit NF-κB signal pathway and prevent osteoclastogenesis. The primary structure-activity relationship (SAR) study indicates that hydrophilic groups in R_2 and R_3 position of ring A can increase the anti-osteoclastogenesis activity. The docking study also revealed that ring A in a hydrophilic pocket. Here, the SAR study of ring B was not applied, the

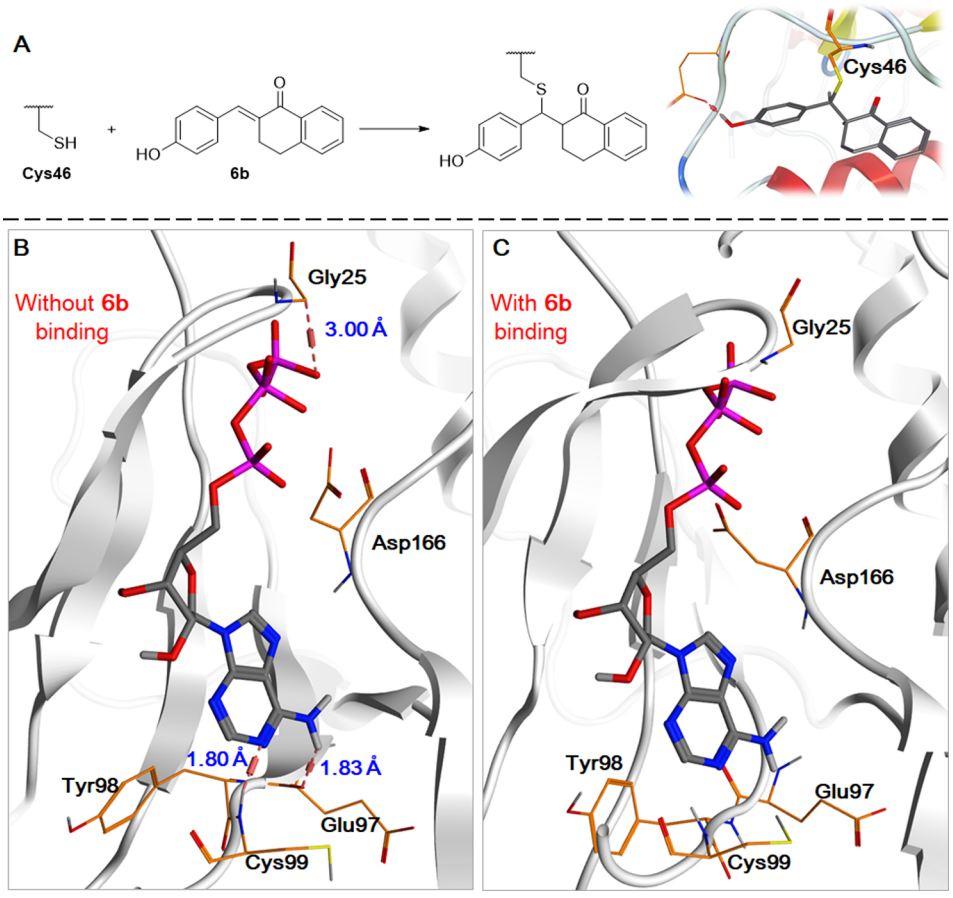

Fig. 9. (A) The covalent binding of compound **6b** and IKKβ at Cys46. (B) The binding complex of IKKβ-ATP without **6b**. (C) The binding complex of IKKβ-ATP with **6b**. H-bonds are represented as orange dashed lines. The ribbon and amino acids of IKKβ-**6b** are represented as yellow color. The ribbon and amino acids of IKKβ-ATP are represented as blue color. (For interpretation of the references to color in this figure legend, the reader is referred to the web version of this article.)

modification on ring B will be performed in future to improve activity. According to the docking study, the ring B fits into a hydrophobic pocket, introducing hydrophobic groups may improve the potency of compounds. Bioassay results indicated that compound **6b** selectively prevent RANKL-induced NF-κB signal pathway without affecting RANKL-induced MAPK and PI3K/Akt pathway. Further docking study suggests that **6b** may covalent bind with IKKβ to block NF-κB function. However, more bioassay is needed to study its mechanism of action.

3. Conclusion

In conclusion, compound **6** contains α,β–unsaturated enone moiety, was identified as a potential anti-osteoporosis scaffold. Twelve derivatives were founded from in-house library. Among them, compound **6b** exhibited most potent inhibitory effects of RANKL-induced osteoclastogenesis in BMMs without cytotoxicity, as well as inhibition of bone resorption *in vitro*. The ALP staining indicated **6b** has no effect on osteoblast function. Thus, compound **6b** selectivity inhibits osteoclast differentiation. Compound **6b** also inhibits NF-κB signaling pathway and affect NF-κB targeted gene expression including TRAP, c-Fos, MMP9, and NFATc1. A docking study indicated **6b** may block NF-κB activity through covalent binding with IKKβ. Therefore, **6b** could be a lead compound for further study.

4. Material and methods

4.1. Reagents and antibodies

All the compounds are obtained from SYSU small molecular repository center. Compound **6** can be prepared by using previous reported method [26]. **JSH23** is purchased from MCE (USA). α-Modified Minimal Essential Medium (α-MEM), Dulbecco's Modified Eagle's Medium (DMEM), Phosphate buffered saline (PBS) and fetal bovine serum (FBS) were purchased from Gibco (Gibco, NY, USA). MTS reagent and luciferase analysis reagents were purchased from Promega (Promega Corporation, Sydney, Australia). Primary antibodies for p65, phosphorylated p65, IκB-α, ERK, phosphorylated ERK, JNK, phosphorylated JNK, p38, phosphorylated p38, PI3K, phosphorylated PI3K, Akt and phosphorylated Akt were obtained from Cell Signaling Technology (Cell Signaling Technology, Massachusetts, USA). All antibodies were used at the concentrations recommended by the supplier at 1:1000. Recombinant macrophage colony stimulating factor (M-CSF) was obtained from R&D Systems (Minneapolis, MN, USA). Hydroxyapatite-coated 24 well plates were obtained from Corning (Corning, USA). Acid Phosphatase Leukocyte (TRAP) kit, cell dissociation solution and 5-bromo-4-chloro-3-indolyl phosphate/nitro blue tetrazolium (BCIP/NBT) solution were obtained from Sigma Aldrich (Sigma Aldrich, St Louis, MO, USA). TRIzol reagent was obtained from Invitrogen (Invitrogen, NY, USA). PrimeScript™ MixRT Master Mix reverse transcriptase kit and TB Green™ premix EX Taq™ II kit were obtained from Takara (Takara Biotechnology, Kusatsu, Japan). Glutathione S-transferase (GST)-rRANKL160–318 (GST-rRANKL) recombinant protein was expressed and purified as previously described [27].

4.2. Cell culture

RAW264.7 cells (mouse macrophage cells) was obtained from America Type Culture Collection (Mannassasa, VA, USA) and maintained in complete α-MEM (α-MEM, 10% heat inactivated FBS, 2 mM L-glutamine and 100 U/mL penicillin/streptomycin). C2C12 cells was maintained in complete DMEM (DMEM, 10% heat inactivated FBS, 100 U/mL penicillin/streptomycin). Cultured the cells in 5% CO_2 at 37 °C.

4.3. Luciferase reporter gene assay for NF-κB

For measuring the effect of compounds on NF-κB transcriptional activation, luciferase reporter gene assays were used. RAW 264.7 cells stably transfected with an NF-κB luciferase reporter gene (3κB-Luc-SV40) [28] were seeded into 96-well plates at a density of 1.5×10^5 cell/well. Pretreated compounds at 0.1, 0.3, 1, 3, 10, 30 μM concentrations for 1 h, and then stimulated with GST-rRANKL (100 ng/mL) for 4 h. Cells were then lysed, and luciferase activity was measured using a Promega Luciferase Assay system.

4.4. Osteoclast differentiation assay

RAW264.7 were seeded at a density of 6×10^3 cell/well onto a 96-well plate and stimulated with M-CSF (30 ng/mL) and GST-rRANKL (100 ng/mL), with or without different concentrations of compounds (0.1, 0.3, 1, 3, 10, 30 μM). The medium, GST-rRANKL and compounds were replaced every 2 days. After 5 days, fixed the cultures with 4% paraformaldehyde in PBS for 15 min at room temperature (r.t.) and then washed four times with PBS. Detection of TRAP activity was performed using the Acid Phosphatase Leukocyte kit and the number of TRAP positive multinucleated cells (more than three nuclei) were counted using a Leica microscope.

4.5. In vitro osteoclastogenesis assay

BMMs were isolated from six-week-old C57BL/6J mice by flushing the marrow from the femur and tibia. Cells were then cultured in α-MEM supplemented with 10% FBS, 2 mM L-glutamine, 100 U/mL penicillin, and 100 μg/mL streptomycin (complete medium), in the presence of M-CSF (30 ng/mL). To generate osteoclasts, BMMs were plated in 96-well plates at a density of 6×10^3 cells/well in the presence of M-CSF (30 ng/mL) overnight. The following day, cells were then stimulated with complete medium containing M-CSF and GST-rRANKL (100 ng/mL) in the presence or absence of compound **6b** (0.03, 0.1, 0.3, 1, 3, 10 μM) every 2 days until osteoclasts formed. After 5 days, cells were fixed with 4% paraformaldehyde for 15 min at r.t. and then stained for TRAP enzymatic activity using Acid Phosphatase Leukocyte kit, following the manufacturer's procedures. TRAP-positive multinucleated cells (> 3 nuclei) were counted as osteoclast-like (OCL) cells.

4.6. Cytotoxicity assay

A CCK-8 assay was used to determine cell viability. BMMs and C2C12 cells in the logarithmic growth phase were cultured in 96-well plates with 6×10^3 cells in each well and incubated for 24 h. The cells were then treated with DMSO vehicle or with different concentrations of compounds ranging from 0.1 μM to 33 μM for 48 h or 72 h. After the treatment period, 10 μL CCK-8 was added to each well, wells were incubated at 37 °C for 30 min, and absorbance was then measured at 450 nm using a microplate reader (Thermo, USA).

4.7. Hydroxyapatite resorption assay

BMMs (1×10^5 cells/well) were cultured onto 6-well collagen-coated plates and stimulated with GST-rRANKL and M-CSF (30 ng/mL) until mature osteoclasts formed. Cells were gently harvested using cell dissociation solution and consistent numbers of mature osteoclasts were seeded into hydroxyapatite-coated 24 well plates. Mature osteoclasts were incubated in medium containing GST-rRANKL and M-CSF with or without compound **6b**. After 48 h, wells were bleached to remove cells, followed by image acquisition for the measurement of resorbed areas using a Leica inverted microscope (Leica, Germany). The percentage of surface resorbed was analyzed using Image J software (NIH, Bethesda, USA).

4.8. Real time polymerase chain reaction (RT-qPCR)

For Real-Time PCR, BMMs were seeded in a 6-well plate at a density of 1×10^5 cells per well and then cultured in complete α-MEM with M-CSF (30 ng/mL), GST-rRANKL (100 ng/mL), and with or without compound **6b** at 5 μM for 5 days. For RT-qPCR analysis, total cellular RNA was extracted cultured cells with TRIzol reagent, following the manufacturer's protocol. Reverse transcription was performed using PrimeScript™ MixRT Master Mix reverse transcriptase kit, according to the manufacturer's specifications. RT-qPCR was performed using TB Green™ premix EX Taq™ II kit with 1 μL reverse transcriptase for 40 cycles of 95 °C for 10 s, 56 °C for 10 s and 72 °C for 30 s. Primer sequences are as follows:

		Sequences
18s	Forward	5′-CGGCTACCACATCCAAGGAA-3′
	Reverse	5′-GCGGAATTACCGCGGCT-3′
NFATc1	Forward	5′-CAACGCCCTGACCACCGATAG-3′
	Reverse	5′-GGCTGCCTTCCGTCTCATAGT-3′
c-Fos	Forward	5′-CCAGTCAAGAGCATCAGCAA-3′
	Reverse	5′-AAGTAGTGCAGCCCGGAGTA-3′
MMP9	Forward	5′-CCTACTCTGCCTGCACCACTAAA-3′
	Reverse	5′-CTGCTTGCCCAGGAAGACGAA-3′
TRAP	Forward	5′-GGCTATGTGCTGAG-3′
	Reverse	5′-GGAGGCTGGTCTTA-3′

4.9. Western blot assay

RAW264.7 cell lines were grown in 6-well plates at a density of 5×10^5 cells per well. Cells were then pretreated with 5 μM compound **6b** for 4 h and then stimulated with GST-rRANKL (100 ng/mL) for 5, 10, 30 and 60 min. Cells were then lysed with radioimmunoprecipitation (RIPA) Lysis Buffer under ice bath, and pelleted by centrifugation (14,000*g* for 5 min). Transferred cleared lysates into a fresh tube and measured protein concentrations by BCA assay. Same amounts of protein samples were mixed with SDS-polyacrylamide gel electrophoresis (SDS-PAGE) loading buffer and heated at 100 °C for 10 min. Then, loaded samples onto a 10% acrylamide gel and separated using SDS-PAGE. Separated samples were transferred onto a nitrocellulose membrane and incubated in 5% skim milk powder diluted in 1× TBS-Tween (TBST) for 2 h at r.t. Membranes were then incubated with specific primary antibodies (1:1000) at 4 °C, with shaking, overnight. Primary antibody binding was detected using horseradish peroxidase conjugated secondary antibodies (1:5000) coupled with enhanced chemiluminescence (ECL) reagents and visualized on Tanon 5200.

4.10. ALP staining

For ALP staining, C2C12 cells were treated with BMP-2 (10 ng/mL) in presence or absence of compound **6b** (0.01, 0.1, 1, 10 μM) for 6 days, then fixed in 4% paraformaldehyde for 15 min at r.t., rinsed with PBS and stained with BCIP/NBT solution (300 μg/mL) overnight at r.t.

4.11. Molecular docking

For the docking studies, Molecular Operating Environment 2014.10 (MOE, Chemical Computing Group Inc. Montreal, Canada) was used, operating on Windows 10 on a DELL computer (Intel i5, 2.8 GHz CPU, 8 GB memory). The structures of compounds were drawn in MOE package with standard bond lengths and angles, and minimized using the conjugate gradient method. The Gasteiger-Huckel charge was applied for the minimization process, with a distance-dependent dielectric function. A preliminary docking study was carried out using the crystal structure of IKKβ (PDB code: 3QA8). The structure was polished as follows: all water molecules were removed from the crystal structure. The protein was then analyzed using the QuickPrep Tool in MOE. Cys46, Glu49, Arg55, Trp58, Ile62, Val79 and Leu91 were selected as binding site. The docking was performed with all compounds in maximum 30 poses.

To analyze the covalent binding of compound **6b** and IKKβ, we made a single covalent bond between α-C of α,β–unsaturated enone at compound **6b** and the thiol group at Cys46 using MOE. Then, we minimized the binding complex with AMBER99 force field. The IKKβ-ATP complex was adopted from Ref. [29].

Acknowledgements

This work was funded in part of Natural Science Foundation of China (81573310, 81473138, 81803361), GD-NSF (2018A030310143), Western Australia Medical & Health Research Infrastructure Fund, Arthritis Australia foundation, The University of Western Australia (UWA) Research Collaboration Awards, and the Australian Health and Medical Research Council (NHMRC, No 1107828, 1127156).

References

[1] T.D. Rachner, S. Khosla, L.C. Hofbauer, Osteoporosis: now and the future, Lancet 377 (2011) 1276–1287, https://doi.org/10.1016/S0140-6736(10)62349-5.
[2] W.J. Boyle, W.S. Simonet, D.L. Lacey, Osteoclast differentiation and activation, Nature 423 (2003) 337–342, https://doi.org/10.1038/nature01658.
[3] J.G. Allen, C. Fotsch, P. Babij, Emerging targets in osteoporosis disease modification, J. Med. Chem. 53 (2010) 4332–4353, https://doi.org/10.1021/jm9018756.
[4] J.M. Delaisse, T.L. Andersen, M.T. Engsig, K. Henriksen, T. Troen, L. Blavier, Matrix metalloproteinases (MMP) and cathepsin K contribute differently to osteoclastic activities, Microsc. Res. Tech. 61 (2003) 504–513, https://doi.org/10.1002/jemt.10374.
[5] M. Asagiri, K. Sato, T. Usami, S. Ochi, H. Nishina, H. Yoshida, I. Morita, E.F. Wagner, T.W. Mak, E. Serfling, H. Takayanagi, Autoamplification of NFATc1 expression determines its essential role in bone homeostasis, J. Exp. Med. 202 (2005) 1261–1269, https://doi.org/10.1084/jem.20051150.
[6] C.P. Cheng, H.S. Huang, Y.C. Hsu, M.J. Sheu, D.M. Chang, A benzamide-linked small molecule NDMC101 inhibits NFATc1 and NF-kappaB activity: a potential osteoclastogenesis inhibitor for experimental arthritis, J. Clin. Immunol. 32 (2012) 762–777, https://doi.org/10.1007/s10875-012-9660-9.
[7] A. Chatterjee, S. Dasgupta, D. Sidransky, Mitochondrial subversion in cancer, Cancer Prev. Res. (Phila.) 4 (2011) 638–654, https://doi.org/10.1158/1940-6207.CAPR-10-0326.
[8] M.S. Hayden, S. Ghosh, Shared principles in NF-kappaB signaling, Cell 132 (2008) 344–362, https://doi.org/10.1016/j.cell.2008.01.020.
[9] B. Zhou, R.Q. Cron, B. Wu, A. Genin, Z. Wang, S. Liu, P. Robson, H.S. Baldwin, Regulation of the murine Nfatc1 gene by NFATc2, J. Biol. Chem. 277 (2002) 10704–10711, https://doi.org/10.1074/jbc.M107068200.
[10] D. Karasik, F. Rivadeneira, M.L. Johnson, The genetics of bone mass and susceptibility to bone diseases, Nat. Rev. Rheumatol 12 (2016) 496, https://doi.org/10.1038/nrrheum.2016.118.
[11] S.L. Kim, S.H. Kim, Y.R. Park, Y.C. Liu, E.M. Kim, H.J. Jeong, Y.N. Kim, S.Y. Seo, I.H. Kim, S.O. Lee, S.T. Lee, S.W. Kim, Combined parthenolide and balsalazide have enhanced antitumor efficacy through blockade of NF-kappaB activation, Mol. Cancer Res. 15 (2017) 141–151, https://doi.org/10.1158/1541-7786.MCR-16-0101.
[12] R. Wang, Y. Wang, Z. Gao, X. Qu, The comparative study of acetyl-11-keto-beta-boswellic acid (AKBA) and aspirin in the prevention of intestinal adenomatous polyposis in APC(Min/+) mice, Drug Discov. Ther. 8 (2014) 25–32.
[13] K. Rashid, S. Chowdhury, S. Ghosh, P.C. Sil, Curcumin attenuates oxidative stress induced NFkappaB mediated inflammation and endoplasmic reticulum dependent apoptosis of splenocytes in diabetes, Biochem. Pharmacol. 143 (2017) 140–155, https://doi.org/10.1016/j.bcp.2017.07.009.
[14] Z. Gao, C. Yu, H. Liang, X. Wang, Y. Liu, X. Li, K. Ji, H. Xu, M. Yang, K. Liu, D. Qi, H. Fan, Andrographolide derivative CX-10 ameliorates dextran sulphate sodium-induced ulcerative colitis in mice: involvement of NF-kappaB and MAPK signalling pathways, Int. Immunopharmacol. 57 (2018) 82–90, https://doi.org/10.1016/j.intimp.2018.02.012.
[15] T. Dong, C. Li, X. Wang, L. Dian, X. Zhang, L. Li, S. Chen, R. Cao, L. Li, N. Huang, S. He, X. Lei, Ainsliadimer A selectively inhibits IKKalpha/beta by covalently binding a conserved cysteine, Nat. Commun. 6 (2015) 6522, https://doi.org/10.1038/ncomms7522.
[16] J.C. Widen, A.M. Kempema, P.W. Villalta, D.A. Harki, Targeting NF-kappaB p65 with a helenalin inspired bis-electrophile, ACS Chem. Biol. 12 (2017) 102–113, https://doi.org/10.1021/acschembio.6b00751.
[17] V.S. Nguyen, X.Y. Loh, H. Wijaya, J. Wang, Q. Lin, Y. Lam, W.S. Wong, Y.K. Mok, Specificity and inhibitory mechanism of andrographolide and its analogues as antiasthma agents on NF-kappaB p50, J. Nat. Prod. 78 (2015) 208–217, https://doi.org/10.1021/np5007179.
[18] S. Wagner, A. Hofmann, B. Siedle, L. Terfloth, I. Merfort, J. Gasteiger, Development

of a structural model for NF-kappaB inhibition of sesquiterpene lactones using self-organizing neural networks, J. Med. Chem. 49 (2006) 2241–2252, https://doi.org/10.1021/jm051125n.
[19] M. Feng, J. Feng, W. Chen, W. Wang, X. Wu, J. Zhang, F. Xu, M. Lai, Lipocalin2 suppresses metastasis of colorectal cancer by attenuating NF-kappaB-dependent activation of snail and epithelial mesenchymal transition, Mol. Cancer 15 (2016) 77, https://doi.org/10.1186/s12943-016-0564-9.
[20] D. Gyori, D. Csete, S. Benko, S. Kulkarni, P. Mandl, C. Dobo-Nagy, B. Vanhaesebroeck, L. Stephens, P.T. Hawkins, A. Mocsai, The phosphoinositide 3-kinase isoform PI3Kbeta regulates osteoclast-mediated bone resorption in humans and mice, Arthrit. Rheumatol. 66 (2014) 2210–2221, https://doi.org/10.1002/art.38660.
[21] J.E. Huh, W.I. Lee, J.W. Kang, D. Nam, D.Y. Choi, D.S. Park, S.H. Lee, J.D. Lee, Formononetin attenuates osteoclastogenesis via suppressing the RANKL-induced activation of NF-kappaB, c-Fos, and nuclear factor of activated T-cells cytoplasmic 1 signaling pathway, J. Nat. Prod. 77 (2014) 2423–2431, https://doi.org/10.1021/np500417d.
[22] Molecular Operating Environment (MOE), C. C. G. I., 1010 Sherbrooke St. West, Suite #910, Montreal, QC, Canada, H3A 2R7, 2016.
[23] M.G. Ruocco, S. Maeda, J.M. Park, T. Lawrence, L.C. Hsu, Y. Cao, G. Schett, E.F. Wagner, M. Karin, I{kappa}B kinase (IKK){beta}, but not IKK{alpha}, is a critical mediator of osteoclast survival and is required for inflammation-induced bone loss, J. Exp. Med. 201 (2005) 1677–1687, https://doi.org/10.1084/jem.20042081.
[24] Q. Liu, H. Wu, S.M. Chim, L. Zhou, J. Zhao, H. Feng, Q. Wei, Q. Wang, M.H. Zheng, R.X. Tan, Q. Gu, J. Xu, N. Pavlos, J. Tickner, J. Xu, SC-514, a selective inhibitor of IKKbeta attenuates RANKL-induced osteoclastogenesis and NF-kappaB activation, Biochem. Pharmacol. 86 (2013) 1775–1783, https://doi.org/10.1016/j.bcp.2013.09.017.
[25] J. Xu, H.F. Wu, E.S. Ang, K. Yip, M. Woloszyn, M.H. Zheng, R.X. Tan, NF-kappaB modulators in osteolytic bone diseases, Cytok. Growth Fact. Rev. 20 (2009) 7–17, https://doi.org/10.1016/j.cytogfr.2008.11.007.
[26] B. Teng, W. Chen, S. Dong, C.W. Kee, D.A. Gandamana, L. Zong, C.H. Tan, Pentanidium- and bisguanidinium-catalyzed enantioselective alkylations using silylamide as bronsted probase, J. Am. Chem. Soc. 138 (2016) 9935–9940, https://doi.org/10.1021/jacs.6b05053.
[27] J. Xu, J.W. Tan, L. Huang, X.H. Gao, R. Laird, D. Liu, S. Wysocki, M.H. Zheng, Cloning, sequencing, and functional characterization of the rat homologue of receptor activator of NF-kappaB ligand, J. Bone Miner. Res. 15 (2000) 2178–2186, https://doi.org/10.1359/jbmr.2000.15.11.2178.
[28] C. Wang, J.H. Steer, D.A. Joyce, K.H. Yip, M.H. Zheng, J. Xu, 12-O-tetradecanoylphorbol-13-acetate (TPA) inhibits osteoclastogenesis by suppressing RANKL-induced NF-kappaB activation, J. Bone Miner. Res. 18 (2003) 2159–2168, https://doi.org/10.1359/jbmr.2003.18.12.2159.
[29] M. Kalia, A. Kukol, Structure and dynamics of the kinase IKK-beta–A key regulator of the NF-kappa B transcription factor, J. Struct. Biol. 176 (2011) 133–142, https://doi.org/10.1016/j.jsb.2011.07.012.